Rapid Report

Local calcium release in mammalian skeletal muscle

Natalia Shirokova, Jesús García* and Eduardo Ríos

*Department of Molecular Biophysics and Physiology, Rush University, 1750 W. Harrison Street, Chicago, IL 60612 and *Department of Physiology and Biophysics, University of Illinois at Chicago, 900 S. Ashland Avenue, Chicago, IL 60607, USA*

(Received 9 July 1998; accepted after revision 10 August 1998)

1. Fluo-3 fluorescence associated with Ca^{2+} release was recorded with confocal microscopy in single muscle fibres mechanically dissected from fast twitch muscle of rats or frogs, voltage clamped in a two Vaseline-gap chamber.

2. Interventions that elicited Ca^{2+} sparks in frog skeletal muscle (low voltage depolarizations, application of caffeine) generated in rat fibres images consistent with substantial release from triadic regions, but devoid of resolvable discrete events. Ca^{2+} sparks were never observed in adult rat fibres. In contrast, sparks of standard morphology were abundant in myotubes from embryonic mice.

3. Depolarization-induced gradients of fluorescence between triadic and surrounding regions (which are proportional to Ca^{2+} release flux) peaked at about 20 ms and then decayed to a steady level. Gradients were greater in frog fibres than in rat fibres. The ratio of peak over steady gradient (R) was steeply voltage dependent in frogs, reaching a maximum of 4·8 at −50 mV ($n = 7$). In rats, R had an essentially voltage-independent value of 2·3 ($n = 5$).

4. Ca^{2+}-induced Ca^{2+} release, resulting in concerted opening of several release channels, is thought to underlie Ca^{2+} sparks and the peak phase of release in frog skeletal muscle. A diffuse 'small event' release, similar to that observed in these rats, is also present in frogs and believed to be directly activated by voltage. The present results suggest that in these rat fibres there is little contribution by CICR to Ca^{2+} release triggered by depolarization, and a lack of concerted channel opening.

During a skeletal muscle action potential, membrane voltage sensors (dihydropyridine receptors, DHPRs) respond to the depolarization causing Ca^{2+} release channels (ryanodine receptors, RYRs) of the sarcoplasmic reticulum to open. The ensuing Ca^{2+} release activates the contractile proteins. Two mechanisms are believed to induce opening of Ca^{2+} release channels: mechanical interactions with DHPRs (Schneider & Chandler, 1973) and Ca^{2+}-induced Ca^{2+} release (CICR, Endo *et al.* 1970; Ríos & Pizarro, 1988; Klein *et al.* 1996; Stern *et al.* 1997). It is believed that in skeletal muscle voltage sensors directly open Ca^{2+} release channels first, and CICR is activated secondarily.

In amphibian skeletal muscle most of the Ca^{2+} release occurs through Ca^{2+} sparks (Tsugorka *et al.* 1995; Klein *et al.* 1996), discrete events mediated by Ca^{2+} (Klein *et al.* 1996; Shirokova & Ríos, 1997), originally demonstrated in cardiac myocytes (Cheng *et al.* 1993). A form of release without resolvable events also exists, which does not require Ca^{2+} as mediator or trigger (Shirokova & Ríos, 1997). We have proposed that this form, which appears to be directly activated by voltage, provides the precursor Ca^{2+} that triggers Ca^{2+} sparks.

Because Ca^{2+} sparks have been found in cardiac, skeletal and smooth muscle (Nelson *et al.* 1995), and they constitute most of the release flux of frog skeletal muscle, one would expect that most of the release flux of mammalian skeletal muscle would be in the form of sparks as well. Sparks have not been demonstrated in mammalian muscle, however, and there are important structural differences between muscles of the two classes of vertebrates. The ratio of RYRs to DHPRs is greater in amphibian muscle (Anderson *et al.* 1994). Additionally, a Ca^{2+} release channel isoform highly susceptible to activation by Ca^{2+} in bilayers (Sutko & Airey, 1996) is expressed in adult amphibian but not mammalian muscles. This, together with the reasonable assumption that RYRs not directly paired with DHPRs should rely on Ca^{2+} for activation, suggests a greater involvement of Ca^{2+}-dependent mechanisms in amphibia.

Functional studies with cut fibres (termed 'whole-cell' in the following to stress their lack of subcellular resolution) also

suggest variance in control mechanisms. In amphibians and mammals, release flux during a sustained depolarization has an early peak and reaches a steady level after 20–40 ms. The ratio (R) of peak and steady levels is greater in the frog than in the rat; additionally, it is markedly voltage dependent in the frog, while it is almost constant in rat muscle (Shirokova *et al.* 1996). Studies in intact fibres activated by action potentials (Hollingworth *et al.* 1996) did not confirm these differences, however: the release flux was similar in frogs and rats, and the degree of decay of release in repeated action potentials was also similar.

To complete our understanding of these hierarchies of Ca^{2+} release, we compared Ca^{2+} signals in mammalian and amphibian skeletal muscle fibres at the local level using confocal microscopy. The differences found are striking.

METHODS

Cell preparation and solutions

Experiments were carried out in cut skeletal muscle fibres from the extensor digitorum longus (EDL) muscle of the rat (*Rattus norvegicus*, Sprague–Dawley) and the semitendinosus muscle of the frog (*Rana pipiens*), voltage clamped in a two Vaseline-gap chamber mounted on the stage of an inverted microscope.

Adult frogs were anaesthetized by immersing in a 15% ethanol solution, then killed by pithing. Female rats (5–8 weeks) were killed by cervical dislocation under deep anaesthesia induced by intraperitoneal injection of pentobarbitone (50–100 mg (kg body wt)$^{-1}$). Fibres were dissected as described for frog muscle by Kovács *et al.* (1983), and for rat muscle by García & Schneider (1993). Frog fibres were studied at sarcomere lengths between 2·8 (slack) and 3·5 μm, while rat fibres were stretched up to 3·6 μm per sarcomere. Mammalian muscle primary culture (myotubes) was prepared from newborn mice as described by Beam & Knudson (1988). Neonate mice were anaesthetized with halothane and decapitated as approved by the American Veterinary Medical Association.

The 'external' solutions contained (mM): for rats, 2 $Ca(CH_3SO_3)_2$, 2 $Mg(CH_3SO_3)_2$, 150 TEA-CH_3SO_3; for frogs, 10 $Ca(CH_3SO_3)_2$, 110 TEA-CH_3SO_3. Both contained 10 mM Hepes, 1 μM TTX, 1 mM 3,4-diaminopyridine and 1 mM 9-anthracene carboxylic acid. The 'internal' solutions contained (mM): for rats, 145 caesium glutamate, 1 or 8 EGTA, 5 glucose; for frogs, 110 caesium glutamate, 1 EGTA, 10 glucose. They also had 5 mM Mg-ATP, 5 mM phosphocreatine, 10 mM Hepes, 0·2 mM fluo-3 (Molecular Probes, Inc., Eugene, OR, USA), and had calcium added for a free $[Ca^{2+}]$ of 100 nM. For localization of T-tubules 10 μM of Di-8-ANEPPS (Molecular Probes, Inc.) were added to the external solution. Solutions were titrated to pH 7 for frogs or 7·2 for rats and adjusted to 270 or 300 mosmol kg^{-1}, respectively. Experiments were performed at room temperature (17–21 °C).

Myotubes were studied in rodent Ringer solution (García & Schneider, 1993) or rat external solutions (above), after incubation for 30 min at room temperature in a Ringer solution with 10 μM of fluo-3 AM (Molecular Probes, Inc., Eugene, OR, USA).

Electrophysiological and fluorescence measurements

Details of chamber design and voltage clamp were given in Kovács *et al.* (1983) and Shirokova & Ríos (1996). The scanning microscope (MRC 1000, Bio-Rad, Hercules, CA, USA) equipped with a ×40, 1·2 NA water-immersion objective lens (Zeiss Inc., Oberkochen, Germany) was used in standard fluo-3 configuration (Shirokova & Ríos, 1997). Images shown represent fluo-3 fluorescence, determined at 2 ms intervals at 768 points of abscissa x_j along a line parallel to the fibre axis. Fluorescence intensity, $F(x,t)$, was normalized to the baseline intensity $F_0(x)$, derived as an average of $F(x,t)$ before the depolarization pulse was applied.

To record fluo-3 and Di-8-ANEPPS fluorescence simultaneously (Shacklock *et al.* 1995), the emitted light was split at 565 nm and the two beams separated further before acquisition, by a 540 nm band-pass filter and a 585 nm long-pass filter. The remnant Di-8-ANEPPS signal was removed from the fluo-3 image at 540 nm by subtraction of a scaled (> 585 nm) image.

RESULTS

Figure 1*A* and *B* are images of fluorescence in rat and frog muscle fibres, respectively, scanned along a line parallel to the fibre axis. Upon depolarization, Ca^{2+}-related fluorescence of fluo-3 increased, revealing Ca^{2+} release.

As seen previously by Tsugorka *et al.* 1995 and Klein *et al.* 1996, depolarization produced Ca^{2+} sparks in the frog. In the rat, by contrast, the depolarizing pulse produced release with a rapid onset and a diffuse pattern, devoid of resolvable discrete events. There was another difference: the banded pattern of resting fluorescence reversed during depolarization in the frog, indicating that free calcium ion concentration increased more in the regions with lower dye concentration, at Z disks, where triad junctions are located (Klein *et al.* 1996). By contrast, in the rat fibre the fluorescence increased more in the regions with higher resting fluorescence and the banded pattern did not reverse.

The reason for this difference is simply that fluo-3 accumulated more in the triadic regions in the rat. This was clarified using a T-tubule marker. Figure 1*C* shows an x–y scan image from a Di-8-ANEPPS-labelled rat fibre, held at −80 mV. Double lines of beaded appearance, regularly spaced by about 1·2 μm, correspond to two transverse tubules located at both edges of each I band. In the same cell fluo-3 was used to simultaneously measure local changes in $[Ca^{2+}]_i$ (Shacklock *et al.* 1995). In panel *D* are linescan images of Di-8-ANEPPS fluorescence (left panel) and normalized fluo-3 fluorescence (right panel) recorded while applying a 200 ms depolarizing pulse to 0 mV. Represented by a red trace is the fluo-3 fluorescence averaged for the duration of the pulse and in black is the Di-8-ANEPPS fluorescence average during the resting interval. The maxima of both curves coincide, indicating that Ca^{2+} release in the rat also occurred in the triadic regions.

Figure 2 illustrates the voltage dependence of the Ca^{2+} signals. At the top are images of normalized fluorescence at −65 and −55 mV in a frog fibre. As seen before, the frequency of sparks increased with voltage (Shirokova & Ríos, 1997). An automatic detection procedure (Cheng *et al.* 1998) identified eighteen events with an amplitude larger than 0·4 units of resting fluorescence in the image at −65 mV, and forty-seven such events at −55 mV.

The traces below each panel are triadic fluorescence gradients (difference in normalized fluorescence between the centre of the triads and the two neighbouring regions of lesser increase) averaged over all triads in the image. The triadic gradient (Tsugorka *et al.* 1995) is proportional to the release flux, which in whole-cell records has an early peak, followed by a much lower steady phase. At −65 mV the triadic gradient reveals only the steady component of release flux whereas at −55 mV it exhibits a large early peak. This difference illustrates clearly the steep voltage dependence of the ratio R between peak and steady release levels, characteristic of frog muscle (Shirokova *et al.* 1996). Note that at −55 mV the triadic gradient decreases slowly during the 'steady' phase, even though the global fluorescence (indicative of global calcium ion concentration) continues to increase.

Panels *C–F* have corresponding images from rat muscle. No discrete events with $\Delta F/F_0 > 0{\cdot}4$ were found at any voltage ($n = 18$). A diffuse release devoid of discrete events was observed instead, similar to that found in frogs at low voltages or under interventions that suppress CICR (Shirokova & Ríos, 1997).

The corresponding triadic gradients, shown below each image, also exhibit a peak and a steady level. Quantitative

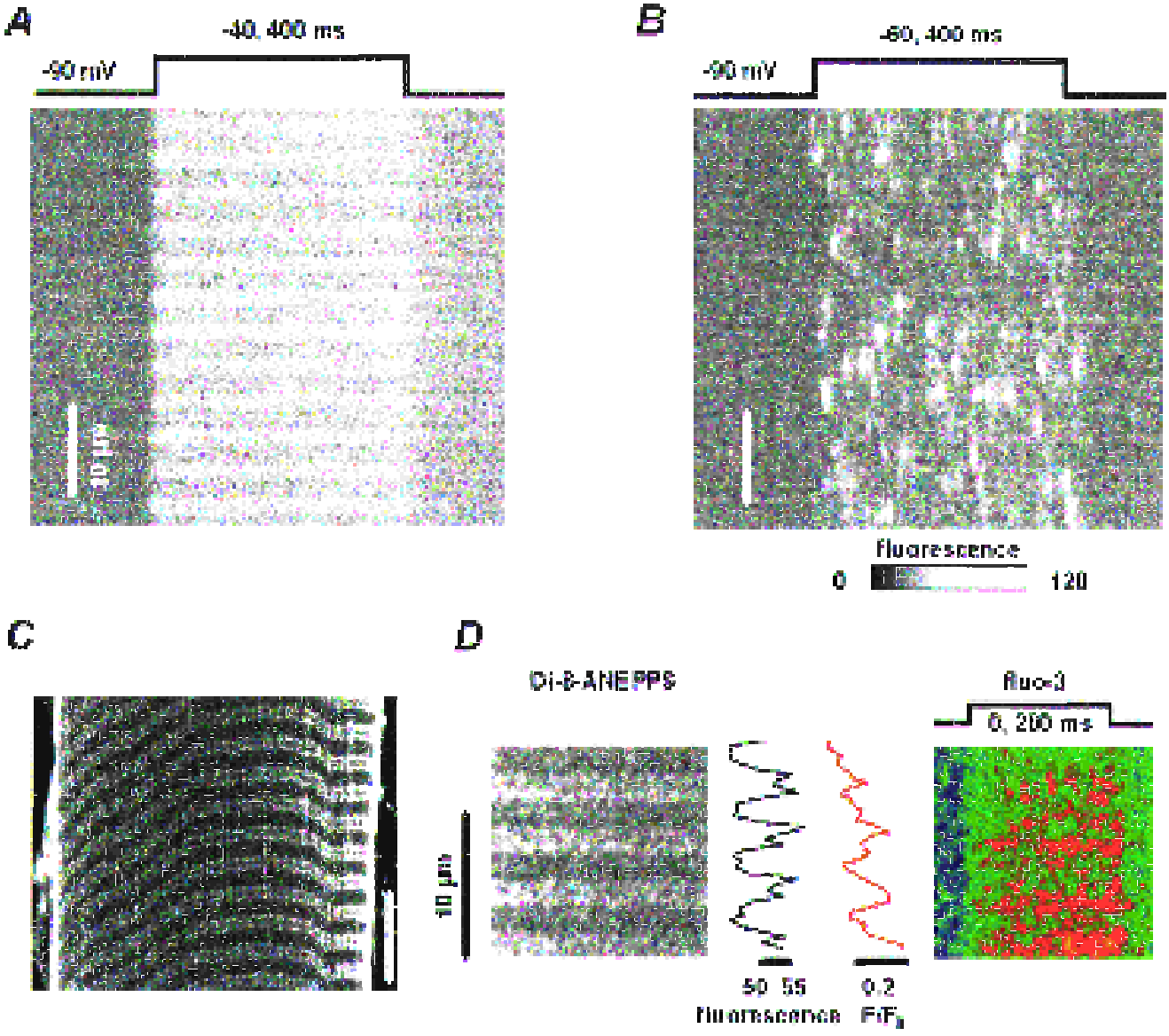

Figure 1. Fluorescence in stimulated frog and rat fibres

Linescan images of fluo-3 fluorescence recorded in rat (*A*) or frog (*B*) fibres upon depolarization as indicated. Optical section of fluorescence in a representative rat fibre (*C*), stained with Di-8-ANEPPS. The double lines correspond to two sets of transverse tubules. *D*, linescan images of Di-8-ANEPPS (left panel, $\lambda > 585$ nm) and normalized fluo-3 fluorescence upon depolarization as indicated. The fluo-3 signal was obtained as the difference of the fluorescence at $\lambda \approx$ 540 nm and a scaled Di-8-ANEPPS signal. More details are given in Methods. Traced in black is the fluorescence of Di-8-ANEPPS averaged during the resting interval. In red is the fluo-3 fluorescence averaged for the duration of the pulse.

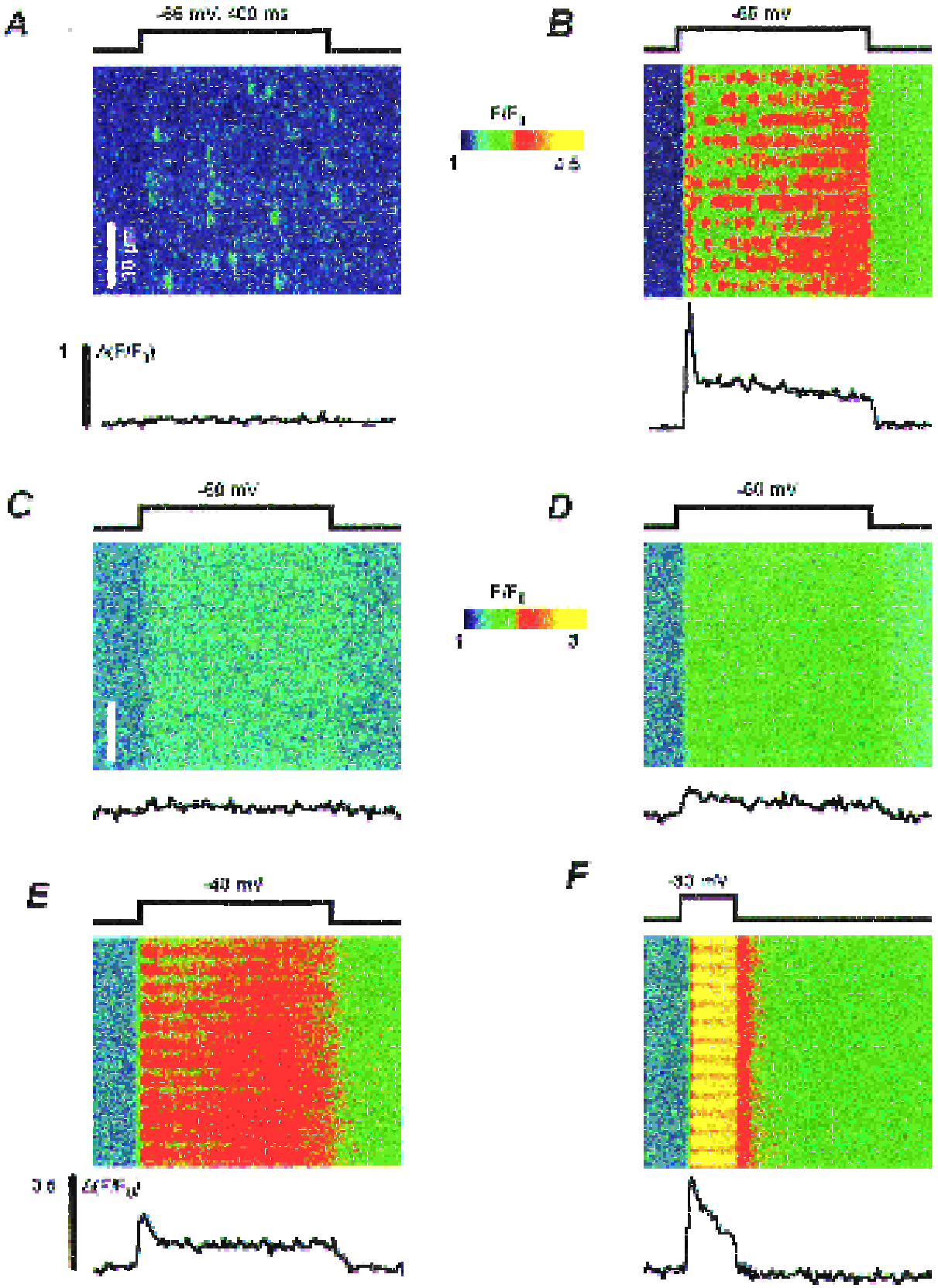

Figure 2. For legend see facing page.

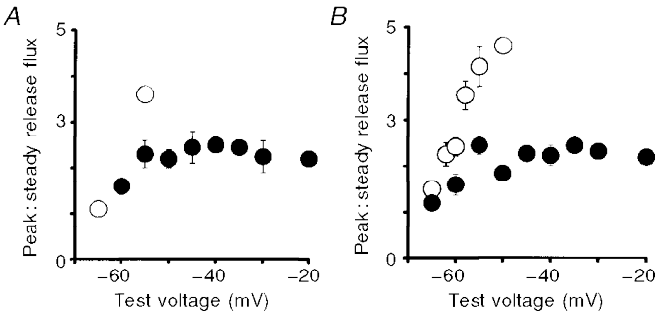

Figure 3. Voltage dependence of peak over steady release flux ratio (R)

A, R values for the rat fibre (●) or the frog fibre (○) illustrated in Fig. 2. *B*, average data from 5 rat fibres (●) and 7 frog fibres (○).

aspects of these gradients are compared in Fig. 3. In panel *A* are R values from the images of Fig. 2 for frog (open symbols) or rat (filled symbols). In panel *B* are averages of data collected from five rat and seven frog fibres that were studied over a wider voltage range and using longer duration pulses to better define R. (Frog fibres were studied at different sarcomere lengths, from slack to moderately stretched, without apparent changes in results.)

In agreement with whole-cell results (Shirokova *et al.* 1996) the ratio (R) in rat fibres averaged 2·3 between −55 and −20 mV and was essentially voltage independent in this range, while in frogs it increased steeply with voltage, reaching about 5 at −50 mV. Due to the large release, it was not possible in the frog to explore local release at higher voltages, at which R decays below the maximum of 5–7 found near −45 mV when studied with the whole-cell technique (Shirokova *et al.* 1996).

Ca^{2+} sparks occur spontaneously in resting frog fibres under certain experimental conditions. It was important to test whether similar conditions would lead to spontaneous sparks in the mammal. The frequency of these events is enhanced by high resting calcium ion concentrations, caffeine (Klein *et al.* 1996), or low $[Mg^{2+}]_i$ (Lacampagne, Klein & Schneider, 1998). In Fig. 4*A* are x–y scan images of a frog fibre held at −90 mV, obtained before the extracellular application of 1 mM caffeine (top) or afterwards, at the times listed in each panel. Fibres prepared in this way did not have spontaneous events; as shown, Ca^{2+} sparks were detected after application of 1 mM caffeine (20 cells).

In Fig. 4*B* are corresponding images of a rat fibre held at −80 mV. Sparks were never observed. Within seconds, exposure to 1 mM caffeine produced transient release without discrete events (6 cells).

The experiments described above were carried out at 17–21 °C. Rat fibres could conceivably have very different local release patterns, including sparks, at 36 °C. The Vaseline-gap method, however, is incompatible with temperatures even close to that level.

The concern about temperature was lessened by the observation of sparks in mammalian myotubes at 17–21 °C. Mice myotubes were loaded with fluo-3 AM and imaged with the confocal microscope. Several types of spontaneous Ca^{2+} release events were observed in resting cells. These included spatially large Ca^{2+} transients, which result in visible contractions and are blocked by TTX, smaller long-lasting events arising repeatedly from the same locations, and brief localized events with all the characteristics of Ca^{2+} sparks. Such events are illustrated in an x–y scan in panel *C* and by three selected regions of linescans in panel *D*. The traces plot the normalized fluorescence averaged within the spatial range indicated by brackets. On average in fifty-five events from six cells the amplitude was 0·94 (S.D. ± 0·05), the full duration at half magnitude was 11·8 ± 1·6 ms and the full width at half magnitude was 2·1 ± 0·3 μm. Such characteristics are similar to those of Ca^{2+} sparks observed in frog fibres and in young C2C12 mouse myotubes (Gyorke & Gyorke, 1996). It is clear therefore that embryonic mammalian cells produce sparks at room temperature.

DISCUSSION

This article constitutes the first study of spatially resolved 'local' Ca^{2+} release in adult mammalian muscle. The studies failed to detect Ca^{2+} sparks, under experimental conditions that produce sparks in frog skeletal muscle. Depolarizing pulses or applications of caffeine generated instead Ca^{2+} signals devoid of resolvable discrete events, originating from regions where transverse tubules are located.

These images are further examples of Ca^{2+}-related signals not organized in sparks or resolvable discrete events. Since such signals correspond to a local Ca^{2+} concentration much lower than that in sparks, the result is consistent with the view that sparks are multi-channel events (Lipp & Niggli,

Figure 2. Voltage dependence of local Ca^{2+} signals

Linescan images of normalized fluo-3 fluorescence in a frog fibre (*A*, *B*) or a rat fibre (*C*–*F*), pulsed as indicated. The line plots are triadic gradients of normalized fluorescence, calculated for the frog as the difference between fluorescence in the triad centres and two flanking regions of lesser increase (Tsugorka *et al.* 1995). For rat fibres, the gradient was calculated as the difference between intensity averaged in 5 or 6 pixels comprising 2 transverse tubules and that in the flanking regions of lower fluorescence. The notation $\Delta(F/F_0)$ is used to represent the calculation.

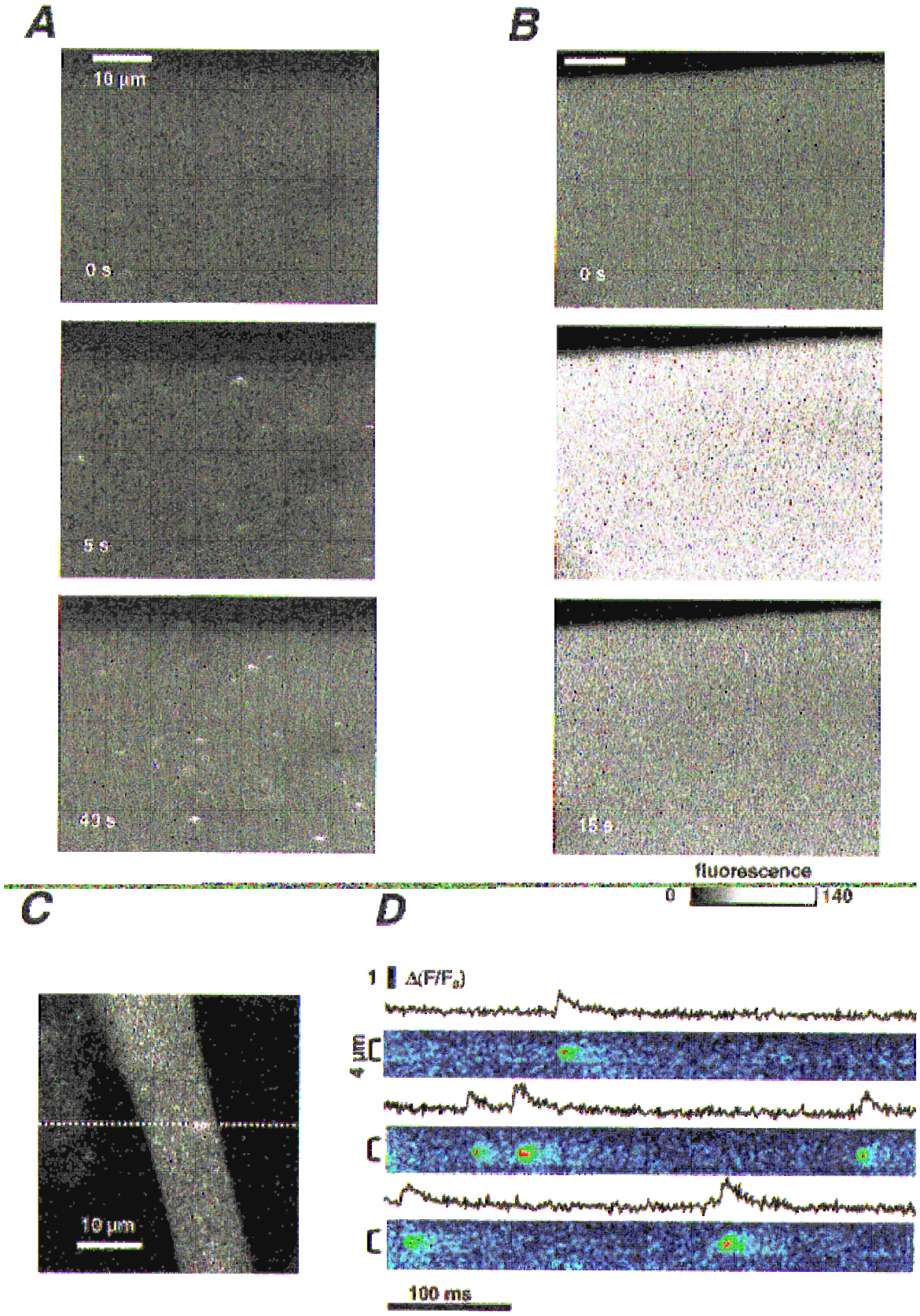

Figure 4. For legend see facing page.

1996). It indirectly supports the proposal that in the frog an event-less release of Ca^{2+}, activated by voltage, provides the trigger for sparks (Shirokova & Ríos, 1997). What in these rat fibres appears to constitute release in its entirety, in frogs could be just a trigger.

Even though the absence of sparks was surprising, the results are consistent with whole-cell determinations of release. Indeed both techniques show release flux with a peak : steady ratio R that in rats is lower, and lacking the voltage dependence it exhibits in frogs. The peak component of Ca^{2+} release is thought to be largely activated by Ca^{2+} (Ríos & Pizarro, 1988) because it is inhibited preferentially by tetracaine (Pizarro *et al.* 1992; Shirokova & Ríos, 1997) and promoted by low intracellular [Mg^{2+}] (Jacquemond & Schneider, 1992). If the steady component of release is more directly related to activation by voltage, then R acquires the meaning of a 'gain' in the amplification contributed by CICR. Both simple and complex models of CICR (Shirokova *et al.* 1996; Stern *et al.* 1997) readily account for R values that are large and voltage dependent. Accordingly, the lower R in the rat is interpreted as evidence of a lesser CICR contribution (Shirokova *et al.* 1996). As CICR is crucial for spark generation (Cheng *et al.* 1993; Klein *et al.* 1996; Shirokova & Ríos, 1997), the observed absence of sparks in the mammal completes a cogent picture of functional differences. On the one hand Ca^{2+} release in frog muscle, largely constituted by sparks, has a large peak and a high and voltage-dependent R. On the other, the rat fibres studied here exhibit release with a lower peak, a lower and voltage-independent R, and absence of sparks. Whatever the reason for these differences might be, the association between a large voltage-dependent R and the presence of sparks strengthens the evidence that both require CICR, and indicates that in these rat fibres CICR is less important.

One might attribute these differences to experimental difficulties with the smaller, more delicate rat cells (e.g. Hollingworth *et al.* 1996). For several reasons, however, these differences between frogs and rats appear to be fundamental rather than circumstantial. L. Csernoch and collaborators (L. Csernoch, P. Szentesi, S. Sárközi, C. Szegedi, I. Jona & L. Kovács, personal communication and manuscript in review) found that tetracaine inhibits peak and steady release equally in mammalian muscle, lacking the high-affinity preferential effect on the peak that it has in the frog (Pizarro *et al.* 1992).

Additionally, there are differences in the molecular make-up of the junction that could determine changes in the control mechanisms. When determined in isolated muscle fractions, ryanodine/DHP specific binding ratio was 1·02 for rabbits and 1·64 for frogs (Anderson *et al.* 1994), indicating that the ratio of RYRs to DHPRs is greater in amphibian muscle. There are also differences in isoform composition. Adult mammalian muscle contains mostly isoform 1 of the RYR. The RYR3 isoform is present at maximal density immediately after birth (Tarroni *et al.* 1997), then decreases during muscle development and differentiation, becoming negligible in adult EDL muscle (Flucher *et al.* 1998). In contrast, an α and a β isoform, homologous to RYR1 and RYR3 (Oyamada *et al.* 1994), are present in equal amounts in chicken (Airey *et al.* 1990) and amphibian skeletal muscle. RYR3 (and β) channels differ from RYR1 (and α) and behave more like the cardiac RYR2 isoform, which is involved in the production of cardiac Ca^{2+} sparks (Sutko & Airey, 1996).

In contrast with the adult cells, developing mouse myotubes exhibit Ca^{2+} sparks. This shows that mammalian cells can produce sparks in our experimental conditions. The result also suggests that RYR3 or β channels may be required for the production of Ca^{2+} sparks, and that without these specific isoforms the role of voltage is enhanced to the detriment of CICR.

This interpretation reconciles other known functional differences between species. RISC (repolarization-induced stop of caffeine contracture; Suda & Penner, 1994) is due to termination upon repolarization of Ca^{2+} release elicited by caffeine. RISC implies that the channels opened by Ca^{2+} (presumably the targets of caffeine) are directly controlled by voltage. RISC was demonstrated in rat and mouse myotubes, but Shirokova & Ríos (1996) failed to find it in frog muscle. This could be another manifestation of fundamental differences between animal classes: in the mammal, RISC reflects a dominant control by voltage, which can overrule any Ca^{2+}-mediated activation. Instead, in the amphibian, some channels appear to be controlled by Ca^{2+} (or caffeine) regardless of the state of the voltage sensor.

In mammals and in tonic muscles of the frog, DHPR tetrads face alternating RYRs along triad junctions (reviewed by Franzini-Armstrong & Jorgensen, 1994). In the frog, the channels not paired with voltage sensors are believed to be opened by CICR (Ríos & Pizarro, 1988), but in mammals the indications of low or absent CICR plus the existence of RISC demand a different trigger. Are the unpaired channels allosterically controlled by sideways interactions in the quasi-crystal of release channels? Are they vestiges of mammalian phylogenesis that do not open under normal stimulation? These questions remain unanswered, but it can

Figure 4. Ligand-induced Ca^{2+} release in adult muscle fibres and developing myotubes

A, x–y scan images of fluo-3 fluorescence in a frog fibre in reference and at the times indicated after introduction of 1 mM caffeine to the bath. *B*, corresponding images from a rat fibre. Application of caffeine produced sparks in frog fibres and diffuse release in rat fibres. *C*, x–y scan image of fluo-3 fluorescence in a mouse myocyte. *D*, normalized images obtained immediately afterwards in the same cell, scanning along the dotted line. Plots represent means of normalized fluorescence in the regions indicated by the brackets, demonstrating sparks with standard properties.

no longer be assumed without demonstration that fundamental mechanisms will be the same in the skeletal muscle of all vertebrates.

Airey, J. A., Beck, C. F., Murakami, K., Tanksley, S. J., Deerinck, T. J., Ellisman, M. H. & Sutko, J. L. (1990). Identification and localization of two triad junctional foot protein isoforms in mature avian fast twitch skeletal muscle. *Journal of Biological Chemistry* **265**, 14187–14194.

Anderson, K., Cohn, A. H. & Meissner, G. (1994). High-affinity [^{3}H]PN200-110 and [^{3}H]ryanodine binding to rabbit and frog skeletal muscle. *American Journal of Physiology* **266**, C462–466.

Beam, K. G. & Knudson, C. M. (1988). Calcium currents in embryonic and neonatal mammalian skeletal muscle. *Journal of General Physiology* **91**, 781–798.

Cheng, H., Lederer, W. J. & Cannell, M. B. (1993). Calcium sparks: elementary events underlying excitation–contraction coupling in heart muscle. *Science* **262**, 740–744.

Cheng, H., Song, L.-S., Shirokova, N., Lakatta, E. G., Stern, M. D. & Ríos, E. (1998). Automated, objective detection and measurement of Ca^{2+} sparks in confocal images. *Biophysical Journal* **74**, A269.

Endo, M., Tanaka, M. & Ogawa, Y. (1970). Calcium induced release of calcium from the sarcoplasmic reticulum of skinned skeletal muscle fibres. *Nature* **228**, 34–36.

Flucher, B. E., Conty, A. & Sorrentino, V. (1998). Type 3 ryanodine receptor is expressed in skeletal muscle triads of developing mice. *Biophysical Journal* **74**, A338.

Franzini-Armstrong, C. & Jorgensen, A. O. (1994). Structure and development of E–C coupling units in skeletal muscle. *Annual Review of Physiology* **56**, 509–534.

García, J. & Schneider, M. F. (1993). Calcium transients and calcium release in rat fast-twitch skeletal muscle fibres. *Journal of Physiology* **463**, 709–728.

Gÿorke, I. & Gÿorke, S. (1996). Adaptive control of intracellular Ca^{2+} release in C2C12 mouse myotubes. *Pflügers Archiv* **431**, 838–843.

Hollingworth, S., Zhao, M. & Baylor, S. M. (1996). The amplitude and time course of the myoplasmic free [Ca^{2+}] transient in fast-twitch fibres of mouse muscle. *Journal of General Physiology* **108**, 455–469.

Jacquemond, V. & Schneider, M. F. (1992). Effects of low myoplasmic Mg^{2+} on calcium binding by parvalbumin and calcium uptake by the sarcoplasmic reticulum in frog skeletal muscle. *Journal of General Physiology* **100**, 137–154.

Klein, M. G., Cheng, H., Santana, L. F., Jiang, Y. H., Lederer, W. J. & Schneider, M. F. (1996). Two mechanisms of quantized calcium release in skeletal muscle. *Nature* **379**, 455–458.

Kovács, L., Ríos, E. & Schneider, M. F. (1983). Measurement and modification of free calcium transients in frog skeletal muscle fibres by a metallochromic indicator dye. *Journal of Physiology* **343**, 161–196.

Lacampagne, A., Klein, M. G. & Schneider, M. F. (1998). Modulation of the frequency of spontaneous sarcoplasmic reticulum Ca^{2+} release events (Ca^{2+} sparks) by myoplasmic [Mg^{2+}] in frog skeletal muscle. *Journal of General Physiology* **111**, 207–224.

Lipp, P. & Niggli, E. (1996). Submicroscopic calcium signals as fundamental events of excitation–contraction coupling in guinea-pig cardiac myocytes. *Journal of Physiology* **492**, 31–38.

Nelson, M. T., Cheng, H., Rubart, M., Santana, L. F., Bonev, A. D., Knot, H. J. & Lederer, W. J. (1995). Relaxation of arterial smooth muscle by calcium sparks. *Science* **270**, 633–637.

Oyamada, H., Murayama, T., Takagi, T., Iino, M., Iwabe, N., Miyata, T., Ogawa, Y. & Endo, M. (1994). Primary structure and distribution of ryanodine-binding protein isoforms of the bullfrog skeletal muscle. *Journal of Biological Chemistry* **269**, 17206–17214.

Pizarro, G., Csernoch, L., Uribe, I. & Ríos, E. (1992). Differential effects of tetracaine on two kinetic components of calcium release in frog skeletal muscle fibres. *Journal of Physiology* **457**, 525–538.

Ríos, E. & Pizarro, G. (1988). Voltage sensors and calcium channels of excitation–contraction coupling. *News of Physiological Sciences* **3**, 223–227.

Schneider, M. F. & Chandler, W. K. (1973). Voltage dependent charge movement of skeletal muscle: a possible step in excitation–contraction coupling. *Nature* **242**, 244–246.

Shacklock, P. S., Wier, W. G. & Balke, C. W. (1995). Local Ca^{2+} transients (Ca^{2+} sparks) originate at transverse tubules in rat heart cells. *Journal of Physiology* **487**, 601–608.

Shirokova, N., García, J., Pizarro, G. & Ríos, E. (1996). Ca^{2+} release from the sarcoplasmic reticulum compared in amphibian and mammalian skeletal muscle. *Journal of General Physiology* **107**, 1–18.

Shirokova, N. & Ríos, E. (1996). Activation of Ca^{2+} release by caffeine and voltage in frog skeletal muscle. *Journal of Physiology* **493**, 317–339.

Shirokova, N. & Ríos, E. (1997). Small event Ca^{2+} release: a probable precursor of Ca^{2+} sparks in frog skeletal muscle. *Journal of Physiology* **502**, 3–11.

Stern, M. D., Pizarro, G. & Ríos, E. (1997). Local control model of excitation–contraction coupling in skeletal muscle. *Journal of General Physiology* **110**, 415–440.

Suda, N. & Penner, R. (1994). Membrane repolarization stops caffeine-induced Ca^{2+} release in skeletal muscle cells. *Proceedings of the National Academy of Sciences of the USA* **91**, 5725–5729.

Sutko, J. L. & Airey, J. A. (1996). Ryanodine receptor Ca^{2+} release channels: does diversity in form equal diversity in function? *Physiological Reviews* **76**, 1027–1071.

Tarroni, P., Rossi, D., Conti, A. & Sorrentino, V. (1997). Expression of the ryanodine receptor type 3 calcium release channel during development and differentiation of mammalian skeletal muscle cells. *Journal of Biological Chemistry* **272**, 19808–19813.

Tsugorka, A., Ríos, E. & Blatter, L. A. (1995). Imaging elementary events of calcium release in skeletal muscle cells. *Science* **269**, 1723–1726.

Acknowledgements

We would like to thank Dr Gonzalo Pizarro for thoughful comments on the manuscript, Drs Roman Shirokov, Adom Gonzalez and Wolfgang Kirsch for helpful discussions, and Eric Nelson for excellent technical help. This work was supported by grants from NIH (R01-AR 32808 and AR 43113 to E.R., T32-HL 07692-07 to N.S.) and MDA USA (to J.G.).

Corresponding author

N. Shirokova: Department of Molecular Biophysics and Physiology, Rush University, 1750 W. Harrison Street, Chicago, IL 60612, USA.

Email: nshiroko@rush.edu

Author's permanent address

N. Shirokova: A. A. Bogomoletz Institute of Physiology, Ukrainian National Academy of Sciences, Bogomoletz Street 4, 252601 GSP, Kiev 24, Ukraine.